NONLINEAR FINITE ELEMENT ANALYSIS OF REINFORCED CONCRETE PLATES

S. BERG, P.G. BERGAN, I. HOLAND

Institutt for Statikk, The Norwegian Institute of Technology, The University of Trondheim, N-7034 Trondheim-NTH, Norway

SUMMARY

This paper is concerned with a numerical method of analysis for reinforced concrete plates. Material and geometrical nonlinearities are included in the computational model so that the behavior may be followed up to the ultimate carrying capacity of the plate. An arbitrary combination of transverse and on inplane loading may be applied to the plate. The method permits the analysis of plates of arbitrary geometric form.

The computational model can account for several layers of reinforcement bars, each of which may have a separate orientation. Any stress-strain diagram may be used for the steel bars. The nonlinear stress-strain relationship for the concrete is accounted for using numerical representation of the results of biaxial tests. Crack initiation in the concrete is considered using experimental failure envelopes.

The Kirchhoff assumptions for thin plates are adopted. Large deflection effects are introduced utilizing the von Kármán strain expressions. Equilibrium and incremental equations accounting for the effects described above are given for the plate.

The general quadrilateral finite elements used in the numerical solution include both inplane and out-of-plane displacements. The stiffness relations for each element are computed numerically by integration based on a set of discrete points distributed over the area and through the thickness of the element. The total system of elements is solved incrementally by applying the external loads in steps. Iterations are also carried out to assure that equilibrium is maintained.

The state of stress is checked at every integration point for each loading step and the material properties at these points are updated accordingly. At points where the cracking limit has been exceeded, cracking is introduced following the direction perpendicular to the axis of the principal tension stress. Previous cracking is memorized.

Computational examples showing the displacements and development of crack patterns in moderately thick concrete slabs are included. Good agreement with experimental results is demonstrated. It is further shown that the geometrical nonlinearities have a significant effect on the behavior at high levels of loading.

1. Introduction

Analysis of reinforced concrete structures taking the real material behavior into account is generally a very complex and difficult problem. The design of concrete structures is usually based on simplified elastic analysis or limit load considerations. Unfortunately, such methods can give only limited information about the overall behavior of the structure in the non-linear range of loading.

Modern numerical solution techniques like the finite element method have opened new possibilities in this field. Effects like cracking of concrete, yielding of reinforcement bars and many other nonlinear effects can be accounted for in such finite element models. In principle, cracking may be introduced by two different techniques. One approach could be to form discrete cracks by disconnecting the concrete on the two sides of the crack. Alternatively, assuming that the cracks are relatively densely distributed, the effect of cracking may be incorporated directly in the stress-strain relations of the concrete. The latter approach will be adopted here. This technique was also utilized in references (1), (2) and (3) whereas discrete cracks were used in (4) and (5).

Further, the present work includes geometric effects due to out-of-plane displacements of the plate. It is demonstrated that these effects are of considerable importance in evaluating the ultimate carrying capacity of reinforced concrete plates.

The present paper is based primarily on the Licentiat Degree Thesis (6) of the first author.

2. Mathematical Formulation

2.1 Nonlinear Equilibrium and Incremental Equations for the Plate

The following derivations are based on a displacement formulation of the finite element method. The displacements at the reference plane of the plate, see Fig. 1, are defined as follows

$$\begin{pmatrix} u_0 \\ v_0 \\ w_0 \end{pmatrix} = \begin{pmatrix} N_u & 0 & 0 \\ 0 & N_u & 0 \\ 0 & 0 & N_w \end{pmatrix} \begin{pmatrix} u \\ v \\ w \end{pmatrix} \qquad (1)$$

Here u, v and w are the nodal displacement parameters associated with the u, v and w displacements. N_u, N_v and N_w are the corresponding interpolation polynomials.

Adopting the Kirchhoff assumptions for thin plates, the displacements at a distance z from the reference plane are

$$\begin{pmatrix} u \\ v \\ w \end{pmatrix} = \begin{pmatrix} u_0 \\ v_0 \\ w_0 \end{pmatrix} - z \begin{pmatrix} w_{,x} \\ w_{,y} \\ 0 \end{pmatrix} = \begin{pmatrix} N_u & 0 & -zN_{w,x} \\ 0 & N_v & -zN_{w,y} \\ 0 & 0 & N_w \end{pmatrix} \begin{pmatrix} u \\ v \\ w \end{pmatrix} \tag{2}$$

where commas denote partial differentation.

Large deflections are taken into account using the von Kármán theory for thin plates (7). The strains can then be expressed as

$$\varepsilon = \begin{pmatrix} \varepsilon_x \\ \varepsilon_y \\ \gamma_{xy} \end{pmatrix} = \begin{pmatrix} u_{,x} \\ v_{,y} \\ u_{,y} + v_{,x} \end{pmatrix} + \frac{1}{2} \begin{pmatrix} w^2_{,x} \\ w^2_{,y} \\ 2w_{,x}w_{,y} \end{pmatrix} \tag{3}$$

$$= \left(B_u,\ B_v,\ -zB_{w1} + \tfrac{1}{2}B_{w3}WB_{w2}\right) \begin{pmatrix} u \\ v \\ w \end{pmatrix}$$

where the following definitions have been used

$$B_u = \begin{pmatrix} N_{u,x} \\ 0 \\ N_{u,y} \end{pmatrix}, \qquad B_v = \begin{pmatrix} 0 \\ N_{v,y} \\ N_{v,x} \end{pmatrix}, \qquad B_{w1} = \begin{pmatrix} N_{w,xx} \\ N_{w,yy} \\ 2N_{w,xy} \end{pmatrix}$$

$$B_{w2} = \begin{pmatrix} N_{w,x} \\ N_{w,y} \end{pmatrix}, \qquad B_{w3} = \begin{pmatrix} N_{w,x} & 0 \\ 0 & N_{w,y} \\ N_{w,y} & N_{w,x} \end{pmatrix}, \qquad W = \begin{pmatrix} w & 0 \\ 0 & w \end{pmatrix} \tag{4}$$

It should be noted that the strain expressions are quadratic functions of the out-of-plane displacement parameters w.

Applying the principle of virtual work, the following equilibrium equations for a single finite element arise

$$\int_{V_e} \left(B_u,\ B_v,\ (-zB_{w1} + \tfrac{1}{2}B_{w3}WB_{w2})\right)^T \sigma \, dV = R_e \tag{5}$$

For simplicity, only the external forces R_e acting at the nodal points have been included in equation (5). The stress vector σ is defined by

$$\sigma = \begin{pmatrix} \sigma_x \\ \sigma_y \\ \tau_{xy} \end{pmatrix} \tag{6}$$

Equation (5) is merely a statement of the equilibrium conditions and it is valid regardless of material behavior.

The incremental form of the equilibrium equations may be derived considering two configurations that are close to each other. Taking the difference between the virtual work equations for these two configurations, the following incremental equations can be deduced when some higher order terms are neglected

$$\int_{V_e} (B_u,\ B_v,\ (-zB_{w1} + B_{w3}WB_{w2}))^T D_I (B_u,\ B_v,\ (-zB_{w1} + B_{w3}WB_{w2}))dV \begin{pmatrix}\Delta u\\ \Delta v\\ \Delta w\end{pmatrix} + \int_{V_e} \begin{pmatrix}0\\ 0\\ B_{w2}^T \bar{\sigma} B_{w2}\end{pmatrix} dV\ \Delta w = \Delta R_e \qquad (7)$$

The Δ denotes the difference between values in the two configurations and $\bar{\sigma}$ is defined by

$$\bar{\sigma} = \begin{bmatrix}\sigma_x & \tau_{xy}\\ \tau_{xy} & \sigma_y\end{bmatrix} \qquad (8)$$

D_I is the incremental stress-strain relationship between the two configurations

$$\Delta\sigma = D_I \Delta\varepsilon \qquad (9)$$

The coefficient matrix which relates the incremental forces and displacements in equation (7) is usually termed the "incremental stiffness matrix". Assuming symmetry of D_I, it is a symmetric matrix which is a function of the current stresses and displacements.

The equilibrium equations (5) and the incremental equations (7) may be used for constructing a wide range of different solution techniques. Equivalent matrices for the whole structure are obtained by standard assemblage procedures.

2.2 Stress-strain Relations for Reinforced Concrete

As will be discussed later, the computation of the integrals defined in equations (5) and (7) will be based on a numerical integration scheme founded on a set of discrete integration points within the element. At every such integration point the stress-strain relations must be updated according to the current state of deformation and the previous load history.

Fig. 2 shows a slice of concrete parallel to the plate surfaces. As long as the slice remains uncracked, the stress-strain relations are based on biaxial tests performed by Kupfer (8). A numerical representation of these tests is used from which stresses and incremental stress-strain relations in the principal directions can be computed according to the current strains (6). These relations are transformed to the global x-y system by a standard transformation (2), (3).

When the crack limit according to the test results has been reached, cracks are introduced in the direction perpendicular to the axis of maximum tensile stress, see Fig. 3. The stress-strain relation is then stated by

$$\begin{pmatrix}\sigma_\alpha\\ \sigma_\beta\\ \tau_{\alpha\beta}\end{pmatrix}^c = \begin{pmatrix}0 & 0 & 0\\ 0 & E_{\beta\beta} & 0\\ 0 & 0 & G\end{pmatrix}\begin{pmatrix}\varepsilon_\alpha\\ \varepsilon_\beta\\ \gamma_{\alpha\beta}\end{pmatrix} = D^c_{\alpha\beta}\varepsilon_{\alpha\beta} \qquad (10)$$

The β-axis coincide with the direction of cracking and $E_{\beta\beta}$ is computed according to uniaxial tests. G is kept proportional to $E_{\beta\beta}$. Equation (10) is also transformed to the global xy-system.

The fact that the concrete between cracks will retain some stiffness in the α-direction suggests that a non-zero value of $E_{\alpha\alpha}$ should be used in equation (10). However, it is very hard to find an accurate value of $E_{\alpha\alpha}$ since it is highly dependent on the specific conditions in the cracks. The effect of $E_{\alpha\alpha}$ is therefore neglected in the present model.

It is further assumed that the concrete is unable to carry any stress when tension cracking in a second direction has occurred. The coefficient matrix in equation (10) is then set equal to zero.

Incremental stress-strain relations for cracked concrete are formed in a similar way except that tangent modulii are used instead of secant values.

The reinforcement bars are assumed to be located in layers parallel to the plate surface, all bars being parallel within each layer. In the numerical treatment the bars are assumed to be closely spaced so that each layer may be treated as a continuum. The stress-strain relation for such a layer is given by

$$\sigma^r_{mn} = \begin{pmatrix}\sigma_m\\ \sigma_n\\ \tau_{mn}\end{pmatrix}^r = \begin{pmatrix}E_s & 0 & 0\\ 0 & 0 & 0\\ 0 & 0 & 0\end{pmatrix}\varepsilon_{mn} = D^r_{mn}\varepsilon_{mn} \qquad (11)$$

Subscript m indicates the direction of the bars, and E_s is the current secant modulus. Also this relation is transformed to the xy-system. Corresponding incremental relations are formulated in a similar manner by replacing E_s by the current tangent modulus for the reinforcement.

2.3 The Finite Element

The interpolation polynomials of equation (1) remain to be defined for the finite element. The out-of-plane displacement function w is chosen to be that of the so-called Q19 plate bending quadrilateral element developed by Clough, Tocher and Felippa (9). This element which satisfies complete internal and external slope continuity, is an assembly of 4 triangular elements, each of which has different displacement expansions in three triangular subregions, see Fig. 4.

A standard isoparametric formulation for quadrilateral elements is used for the inplane displacements N_u and N_v. However, additional displacement functions associated with the displacements of the centroid of the quadrilateral is also utilized, see Fig. 5 and references (10), (6).

Following an approach suggested by Bergan and Clough (10), the stiffness relations of equations (5) and (7) can be computed using a numerical integration scheme based on the centroidal points of the twelve triangular subregions of one quadrilateral element. The area of the surrounding subregion is thus associated with such an integration point. Also, Gaussian integration is carried out through the thickness of the plate at these centroids. 3, 5, 7, 9 or 11 points may be used. For problems involving no flexural deformations, only one integration point is necessary through the thickness. For further details, see references (6), (10), (11).

2.4 Solution of The Nonlinear Equations

The nonconservative nature of the concrete material requires the true deformation path be followed closely during the solution procedure. At the same time, the equilibrium equations should be satisfied as well as possible. These two requirements indicate that the best solution technique is to apply the load in increments and iterate to satisfy equilibrium. A Newton-Raphson type iteration is chosen. The incremental stiffness equation (7) is used as gradient matrix both for the load incrementation and for the iterations. As a rule, this gradient may be kept constant during several cycles. Acceleration factors are also used in order to speed up the convergence of the equilibrium iterations. The specific combination of load incrementation and iterations that should be utilized depends on the particular problem to be solved (6).

3. Numerical Examples

3.1 Simply Supported Beam

A simply supported beam subjected to a concentrated load at the midspan was analyzed both as a plate bending and as a plane stress problem. The geometry of the beam and the material properties are given in Fig. 6. The same problem has previously been studied by Franklin (12), whose results will be used for comparison.

Half of the beam was idealized by 3 plate bending elements which also included inplane displacements. Nine Gaussian points through the thickness were used for the integration. Further, the beam was also analyzed using a 3 by 4 plane stress finite element mesh, see Fig. 8. In both cases, a load incrementation technique combined with equilibrium iterations was utilized.

The results obtained for the midpoint deflection are shown in Fig. 7. On the whole, the results agree quite well with the experiments. The discrepancies between the computational and the test results just above load of initial cracking is believed to be primarily caused by insufficient informa-

tion about the modulus of rupture. For higher load levels there are also other factors which may cause inaccuracies in the results. The most important of these are probably the effects of neglecting stresses in the concrete between cracks and disregarding bond slip. Also, cracks propagate more easily in the real beam because of stress concentrations at the tip of the cracks.

The ultimate load of the test beam was limited by diagonal tension cracking. The present plate bending model is capable only of representing cracks normal to the midsurface of the plate. The beam strength was therefore overestimated in this model. A similar behavior was experienced in the plane stress model which also was incapable of representing the large deformations occurring in the diagonal cracks. Better agreement with the tests probably would have been obtained by neglecting the shear resistance of cracked concrete. However, this would give too little stiffness for lower levels of loading.

The development of cracked zones obtained by the two models is shown in Fig. 8. The results are generally good although the plate bending model gives cracks that are too shallow and a cracked zone which extends a bit too close the supports. The fact that bond slip was neglected in the computational model is believed to be the reason for these discrepancies. The cracked zone of the plane stress model seems to be quite good except for that a few local areas disturb the picture somewhat. However, it should be remembered that the finite element meshes that have been utilized are very coarse and that more accurate results could be expected for finer mesh idealizations.

3.2 Simply Supported Rectangular Plate

Fig. 9 shows the geometry and the material properties of a plate tested by Taylor, Maher and Hayes (13). The plate was first analyzed without taking the geometric nonlinear effects into account. Thereafter a computation in which these effects were included was carried out. Because of double symmetry, only one quarter of the plate was analyzed using a 2 by 2 mesh. Seven Gaussian points were used for the integration through the thickness. A uniform pressure was applied incrementally to the plate, each increment being equal to half of the load of initial cracking. Iterations for obtaining equilibrium was performed after each load increment.

The midpoint deflection during loading is shown in Fig. 10. Very good agreement with the test results was obtained for the load of initial cracking. However, the analysis gave deflections which were too large during the following load increments. This was probably caused mainly by neglecting the modulus $E_{\alpha\alpha}$, see Section 2.2.

When the effects due to geometric nonlinearities were neglected, the ultimate load obtained was close to the value resulting from the yield line theory, see Fig. 10. The yield moment in the yield line analysis was based on plastic flow of the reinforcement and a rectangular stress distribution in the compression zone of the concrete with a stress equal to the uniaxial

compressive strength.

When the changes in the geometry were accounted for, the computed results came out very close to the experimental curve for load levels higher than twice the load of initial cracking. One effect of the geometrical nonlinearities is that cracking will occur through the entire thickness of the plate. This phenomenon was observed during testing (13) as well as in the numerical computations.

The inplane displacements at the midside points are shown in Fig. 11. The cracking led to outward displacements while the geometric nonlinearities had the opposite effect. This is very clearly demonstrated by the two curves.

Crack patterns for different levels of loading are shown in Fig. 12. The results seem to be in good agreement with what could be expected. However, some of the directions of cracking are hard to explain. Probably the performance could be improved by using smaller load increments and finer element mesh.

4. Conclusions

A computational model for nonlinear analysis of reinforced concrete plates has been developed. This model accounts for nonlinear stress-strain relations both for reinforcement and concrete. Further, cracking of concrete is taken into account by modifying the stress-strain relations. Changes in the geometry caused by large deflections are also included in the analysis. The model is general in that plates with different geometry, different support conditions and with several reinforcement layers oriented in arbitrary directions may be analyzed.

Good agreement with experimental results have been obtained by the present method. However, there are several factors that complicate calculations of this type. First, more knowledge about the behavior of concrete under general biaxial states of stress is urgently needed. Another difficult point is to find simple mathematical models for the interaction between concrete and reinforcement bars during cracking and bond slip. Finally, variations of the concrete properties in the real structures due to production conditions etc. set limits for the degree of accuracy that possibly can be obtained by numerical calculations.

References

(1) ISENBERG, J., ADHAM, S., "Analysis of Orthotropic Reinforced Concrete Structures", ASCE Proc., Journal of the Str. Div., Vol. 96, No. ST 12, Dec. 1970.

(2) CERVENKA, V., GERSTLE, K.H., "Inelastic Analysis of Reinforced Concrete Panels", IABSE Publications 31-II, Zürich (1971)

(3) HOLAND, I., MUNKEBY, E., "Analysis of Orthotropic Reinforced Concrete Structures", Discussion, ASCE Proc., Journal of the Str. Div., Vol. 97, No. ST 10, Oct. 1971.

(4) NGO, D., SCORDELIS, A.C., "Finite Element Analysis of Reinforced Concrete Beams", ACI Journal, Proc., Vol. 64, No. 3, March 1967.

(5) NILSON, A.H., "Nonlinear Analysis of Reinforced Concrete by the Finite Element Method", ACI Journal, Proc., Vol. 65, No. 9, Sept. 1968.

(6) BERG, S., "Nonlinear Finite Element Analysis of Reinforced Concrete Plates", Report No. 73-1, Div. of Structural Mech., The Norwegian Institute of Technology, Trondheim, Feb. 1973.

(7) WASHIZU, K., "Variational Methods in Elasticity and Plasticity", Pergamon Press, 1968.

(8) KUPFER, H., "Das Verhalten des Betons unter zweiachsiger Beanspruchung", Bericht Nr. 78, Lehrstuhl für Massivbau, Technische Hochschule, München 1969.

(9) CLOUGH, R.W., FELIPPA, C.A., "A Refined Quadrilateral Element for Analysis of Plate Bending", Proc. 2nd Conf. on Matrix Methods in Structural Mechanics, Wright-Patterson AFB, Ohio 1968.

(10) BERGAN, P.G., CLOUGH, R.W., Elasto-plastic Analysis of Plates Using the Finite Element Method", Proc. 3rd Conf. on Matrix Methods in Structural Mechanics, Wright-Patterson AFB, Ohio 1971.

(11) BERGAN, P.G., "Nonlinear Analysis of Plates Considering Geometric and Material Effects", Ph.D. Dissertation, University of California, Berkeley, March 1971.

(12) FRANKLIN, H.A., "Nonlinear Analysis of Reinforced Concrete Frames and Panels", Ph.D. Thesis, Dep. of Civ. Eng., University of California, Berkeley, March 1970.

(13) TAYLOR, R., MAHER, D.R.H., HAYES, B., "Effect of the Arrangement of Reinforcement on the Behaviour of Reinforced Concrete Slabs", Magazine of Concrete Research, Vol. 98, No. 55, June 1966.

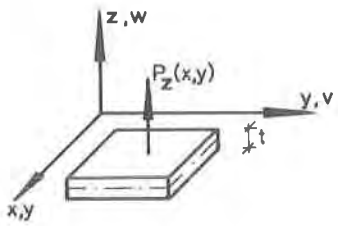

Fig. 1 Reference coordinate system

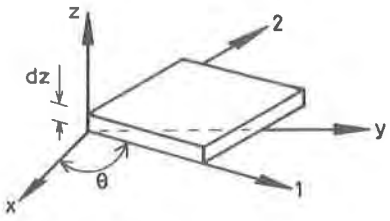

Fig. 2 A slice of concrete

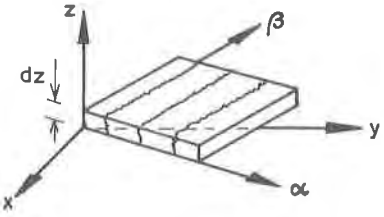

Fig. 3 A concrete subregion with cracks

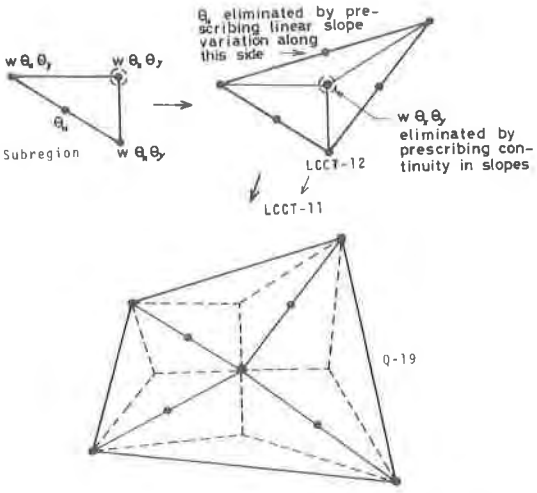

Fig. 4 The Q-19 quadrilateral

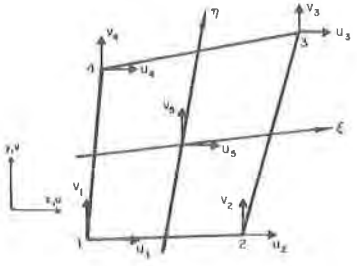

$$N_u^T = N_v^T = \frac{1}{4}\begin{vmatrix} (1-\xi)(1-\eta) - (1-\xi^2)(1-\eta^2) \\ (1+\xi)(1-\eta) - (1-\xi^2)(1-\eta^2) \\ (1+\xi)(1+\eta) - (1-\xi^2)(1-\eta^2) \\ (1-\xi)(1+\eta) - (1-\varepsilon^2)(1-\eta^2) \\ \eta(1-\xi^2)(1-\eta^2) \end{vmatrix}$$

Fig. 5 Inplane displacement field

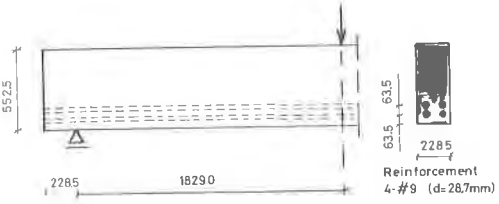

Uniaxial Stress-Strain Relationship

Concrete		Reinforcement	
ε	σ (N/mm²)	ε	σ(N/mm²)
0.0001	0.02295	0	0
0	0	0.002158	4.135
-0.0007	-0.15150	0.005600	6.620
-0.0013	-0.22040	0.020000	9.170
-0.0019	-0.28100	0.060000	9.930
-0.0024	-0.32750		

Fig. 6 Simply supported beam OA-1

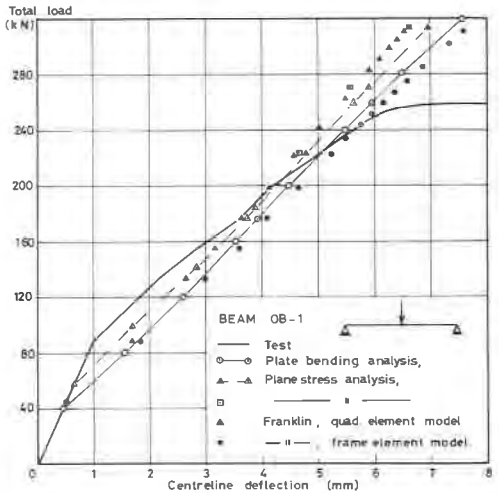

Fig. 7 Load-deflection curves for simply supported beam OB-1

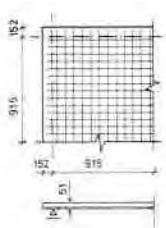

f_c = 35 N/mm²
Reinforcement 476 mm diameter
plain round mild steel
Yield stress 375 N/mm²
Ultimate stress 485 N/mm²
Cover to the bottom layer 476mm

Fig. 9 Simply supported Quadratic Plate

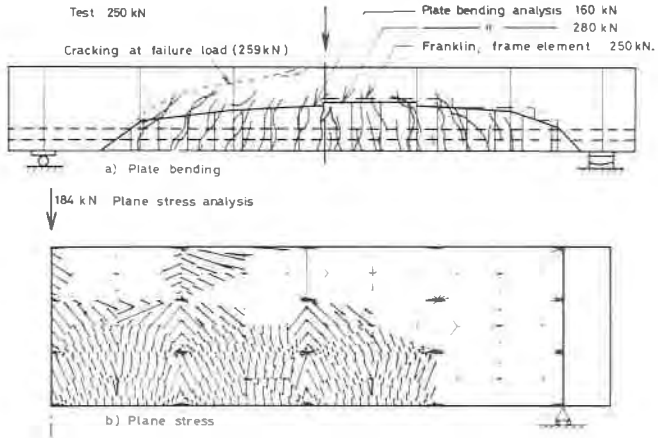

Fig. 8 Simply supported beam OB-1, Crack patterns

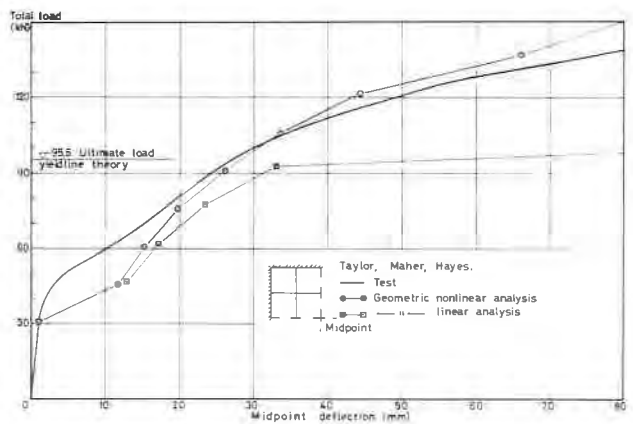

Fig.10 Load-deflection curves for simply supported square plate uniformly loaded

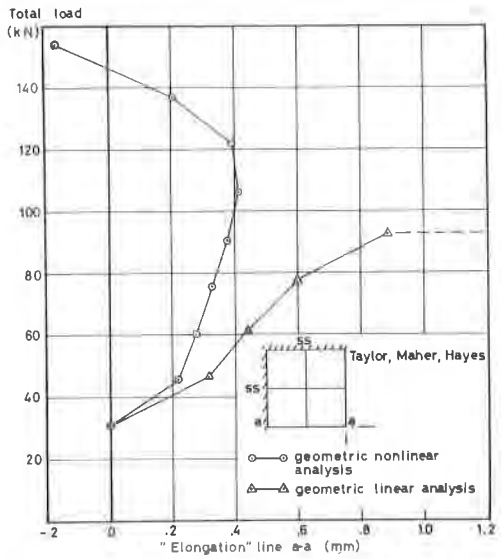

Fig.11 Inplane displacements at the midside points

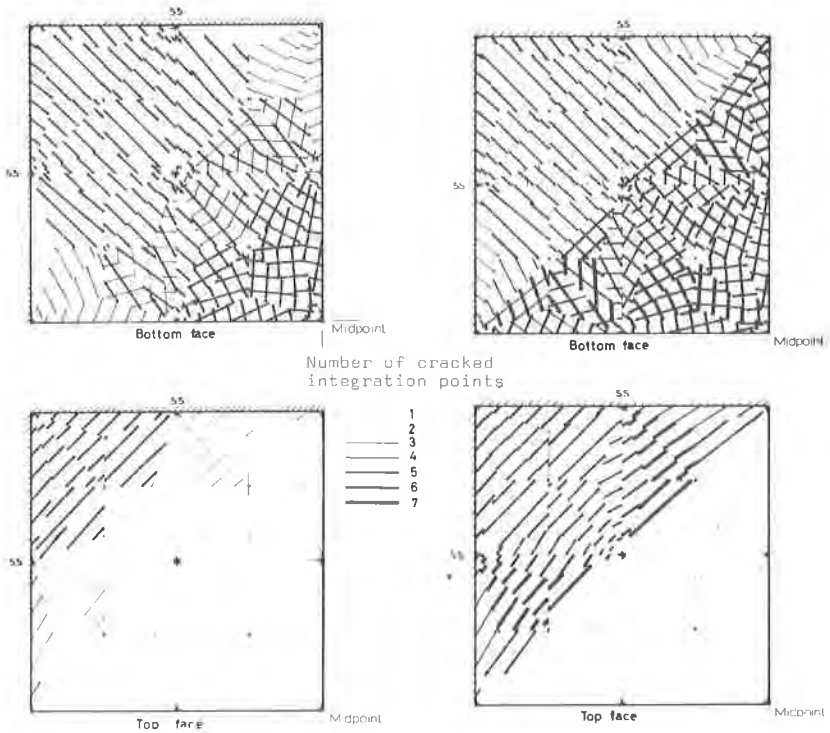

Fig.12 Crack patterns